CHAPTER FOUR

An Alternative Approach to Space Curve Analysis Using the Example of the Neanderthal Occipital Bun

David Paul Reddy, Katerina Harvati, and Johann Kim

INTRODUCTION

In the course of several morphometric analyses that used outlines or curves (also simply called lines, or often "space curves" in three-dimensional), which had been resampled to produce semilandmarks, it became clear to the authors that an alternative to conventional techniques for reducing unwanted variance caused by the placement of semilandmarks at regular intervals along the curves (this variance being considered an artifact of resampling, and therefore neither of biological nor statistical significance) could be devised to take better advantage of the higher density of information in the original unresampled curves.

AQ: Please note that there is a discrepancy in the affiliation provided for David Paul Reddy in the chapter and the Contributor's list. Please confirm the version to be followed.

David Paul Reddy • Vertebrate Paleontology, American Museum of Natural History, 79th St. at Central Park West, New York, NY 10024. **Katerina Harvati** • Department of Anthropology, New York University, 25 Waverly Place, New York, NY 10003. **Johann Kim** • Vertebrate Paleontology, American Museum of Natural History, 79th St. at Central Park West, New York, NY 10024.

Modern Morphometrics in Physical Anthropology, edited by Dennis E. Slice.
Kluwer Academic/Plenum Publishers, New York, 2004.

A remark by F. James Rohlf that such a technique could have advantages, but that it had not yet been implemented, proved to be the catalyst for development of the algorithm presented here and for its application to the re-analysis of data collected by Harvati, which has been the subject of other papers and abstracts (Harvati, 2001; Harvati et al., 2002; Harvati and Reddy, in prep.).

AQ: Please update Harvati and Reddy

Various techniques to minimize extraneous variation along curves as an artifact of resampling have been and are employed in geometric morphometric applications in physical anthropology. Dean et al. made a study of a series of space curves (glabellar and lateral brow ridge, temporal line, coronal suture, and superior nuchal line) considered individually in *Homo erectus* and modern *Homo* using a chi-square test to classify transitional specimens (Dean et al., 1996). A two-step process was used to construct first an average curve by averaging the points obtained by resampling individual splined curves, which had been aligned to best fit at equal intervals of arc length, and then the average curve was splined and resampled at equal intervals of arc length, planes projected orthogonal to the tangents of points resampled at equal arc length on the splined average curve, and the intersections of the original splined curves with these orthogonal planes taken to produce a set of resampled curves with minimized variance. The points on these resampled curves were then averaged within group (*H. erectus* and modern) to produce an average curve for each group. Curves from specimens labeled as transitional were then fit endpoint-to-endpoint with each of the group average curves (though in our opinion this would seem to have the effect of reintroducing some variance along the curve, assuming the curves are not again resampled) and rotated around the chord between the joint endpoints for minimum variance. Summed distances between each transitional curve and the fit and rotated group average curves were calculated and compared to the same statistics calculated within-group, and chi-squared and empirical probabilities used to make assignments of transitional specimens to one of the two groups.

Bookstein et al. undertook a study very similar in aim to the present study, comparing inner and outer mid-sagittal frontal cranial profiles in archaic and modern *Homo* (Bookstein et al., 1999) using Procrustes analysis, sliding, and permutation tests. Bookstein's classic "sliding" technique (Bookstein, 1997) minimizes the mean-squared variance between uniformly sub-sampled or resampled curves which have already been fitted by Generalized Procrustes Analysis (GPA), by allowing the semilandmarks, those resampled points along the curves that are not Type I, II, or III landmarks (Bookstein, 1991), to slide along

the curve. The sliding technique minimizes or "relaxes" the bending energy of the resampled points, using the model known as the "thin-plate spline," which is based on the physics of the deformations of an infinite and infinitely thin plate of metal (Bookstein, 1989). It should be noted that in these studies the curves were deliberately sampled with a uniform number of semilandmarks.

A completed manuscript by Marcus and coauthors applies Bookstein's sliding to ridge curves on fossil and living Papio and Theropithecus (Marcus et al., 2000). In that study landmarks and curves were collected in three-dimensions using a jointed three-dimensional digitizing arm, and the curves were densely and nonuniformly sampled. The curves were subsequently uniformly resampled, and were then projected into the Procrustes space defined by the landmarks alone and slid by Bookstein. The goal of the study was to see what additional information could be gleaned from the statistical analysis of the curves.

What all these studies have in common is that the sliding or relaxation is accomplished on uniformly sub-sampled or resampled curves. The technique proposed in this chapter attempts to provide an alternative to conventional techniques for reducing extraneous variation along resampled curves, accomplishing the same functional goals, while preserving as much fidelity to the original space curve information as possible. While our technique does not require any "typed" landmarks to exist in the input curves, it is advisable to have important features, such as the endpoints of the curve segments, fixed by biologically meaningful landmarks.

MATERIALS

The occipital "bun," or chignon, is one of the most frequently discussed Neanderthal characteristics and often considered a derived Neanderthal trait. The presence of a weak occipital bun, or "hemibun," in many Late Paleolithic European specimens has been seen by some as evidence of continuity or interbreeding between Neanderthals and early modern humans in Europe, particularly in the Central European fossil record and the Mladec crania (see Harvati, in prep. for further citations). The occipital bun is described variably as a posterior projection of the occipital squama or a great convexity of the occipital plane, and is often associated with the presence of a depression of the area around lambda on the occipital and parietal bones. This trait has been applied to a range of morphological patterns and is difficult to assess using

AQ: Yaroch, 1996 not listed in references

either traditional caliper measurements (Dean et al., 1998; Ducros, 1967) or landmark-based geometric morphometrics methods (Harvati, 2001; Yaroch, 1996). It is therefore usually described qualitatively.

Along with the previous work (Harvati, 2001; Harvati et al., 2002; Harvati and Reddy, in prep.), this study evaluates the chignon morphology quantitatively and assesses its usefulness in separating Neanderthals from modern humans, as well as the degree of similarity of the Late Paleolithic "hemibuns" to the Neanderthal occipital buns. This approach uses geometric morphometric analysis of space curves of the midline plane of the posterior part of the skull, which outlines the occipital bun in lateral view. The sample consists of nine recent modern human populations and a fossil sample comprising several Middle and Late Pleistocene hominid specimens. The modern human populations consist of 20–30 individuals each, comprising a total of 255 specimens. Only adult crania were included, as determined by a fully erupted permanent dentition. Sex was unknown in most cases and was assessed by inspection during data collection and from the literature. When possible, equal numbers of male and female specimens were measured. For further details on the recent human samples see Harvati (2001); also Harvati and Reddy (in prep.).

The fossil human sample included nine Neanderthal specimens from Europe and the Near East (Amud 1, Circeo 1, La Chapelle, La Ferrassie 1, La Quina 5, Saccopastore 1, Shanidar 1, Spy 1, Tabun C1); two pre-Neanderthal specimens (Biache, Reilingen); and eight Late Paleolithic anatomically modern humans from Europe (Cro Magnon 1 and 2, Mladec 1, 4, 5, and 6, Predmosti 3 and 4). Where the original fossils were unavailable, high-quality casts from the Anthropology Department of the American Museum of Natural History were measured. As most fossil specimens did not preserve a complete nuchal plane, the analysis was limited to the posterior cranial midline plane from bregma to inion, rather than the complete outline from bregma to opisthion.

While previous studies showed clear distinctions between the mean morphology of modern human, Middle and Late Paleolithic, and Neanderthal populations, some Late Paleolithic specimens were misclassified as Neanderthal when subjected to a discriminant analysis. The present study aims to improve upon the previous results by attempting to increase the fidelity of the data, while maintaining the same degree of sub-sampling and while removing extraneous variation "along the curve" in a manner similar to the Bookstein sliding technique.

THE METHOD

The data for the present study are the same original data as the previous studies (Harvati, 2001; Harvati et al., 2002; Harvati and Reddy, in prep.). They were collected as three-dimensional outline curves composed of landmarks and semilandmarks. All data were collected by Harvati, using the Microscribe 3DX digitizer, with specimens placed in the Frankfurt horizontal plane. Two curve segments were collected in three dimensions between standard osteometric landmarks, from bregma to lambda and from lambda to inion (Figure 3). The two curve segments were resampled so that each specimen comprised the same number of equivalent semilandmarks for each curve segment. To produce the semilandmarks, resampling was done using linear interpolation between original curve points at equal distances along the integrated curve lengths using a custom C program written by Reddy. The two segments were then concatenated, creating a single curve with a total of 25 points, the two endpoints and 23 semilandmarks. This number was chosen by trial-and-error as this was the minimum number that seemed to preserve the visual impression of the original curves. A copy of this data was fit by Generalized Procrustes Analysis (GPA) using Morpheus (Slice, see http://life.bio.sunysb.edu/morph/). This procedure aligns the specimens by translating, rotating, and scaling them for size, so that remaining differences are due to "shape."

Next, the transformation matrix between each set of original, unaligned landmarks and its aligned counterpart was calculated. The affine transformation matrix x of A onto b can be calculated using the "*normal equations*" of linear algebra (Strang, 1976)

$$x = (A^{\mathrm{T}}A)^{-1}A^{\mathrm{T}}b$$

where A is the original, unaligned specimen with an additional dimension whose values are all 1, to convert the resulting matrix from a projection matrix to a transformation matrix, A^{T} is the transpose of the matrix A, and b is the aligned specimen. While the formula is for an affine projection, the constraints imposed by the rigid transformation provided by Morpheus restrict this operation to translation, rotation, and scaling, with no shearing component. The projection or transformation of A onto b is then

$$p = Ax = A(A^{\mathrm{T}}A)^{-1}A^{\mathrm{T}}b.$$

As this procedure was coded in MATLAB, it was both faster computationally and potentially more stable numerically to calculate the transformation matrix using the "mldivide" or backslash operator, which uses QR Factorization to accomplish the same operation, avoiding the matrix inversion step:

$$x = A\backslash b; p = A * x;$$

The unresampled curve for each specimen was then projected by its transformation matrix into the Procrustes space of its resampled counterpart (see Figures 1 and 3). Mean positions for each resampled semilandmark point were calculated from the resampled, GPA'ed curves (see Figures 2 and 4), and mean tangents to the curve were calculated from normalized tangents at points along the unresampled curves closest to the resampled semilandmarks. The endpoints of the curves, anchored at Type I landmarks, were considered fixed and were excluded from these calculations. These mean positions and mean tangents were then used to define perpendicular planes through the data, with the mean positions defining points of rotation for the planes, and the tangents defining normals for the planes.

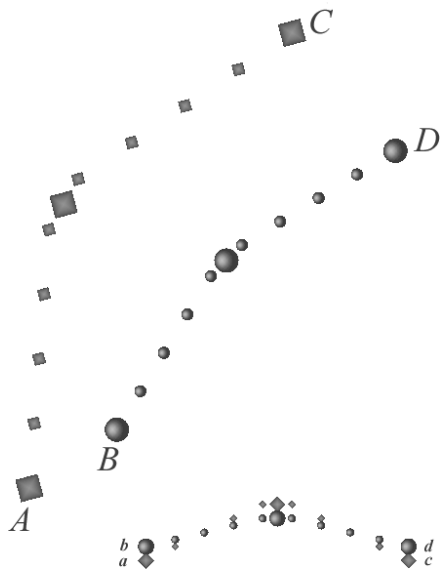

Figure 1. Cartoon of the unresampled points being carried along in a rigid rotation and scaling into Procrustes space with the resampled points. The points on the original curves (small spheres and rhomboids) are carried along with the resampled points (large spheres and rhomboids). The curves AC and BD are projected into the Procrustes space as ac and bd.

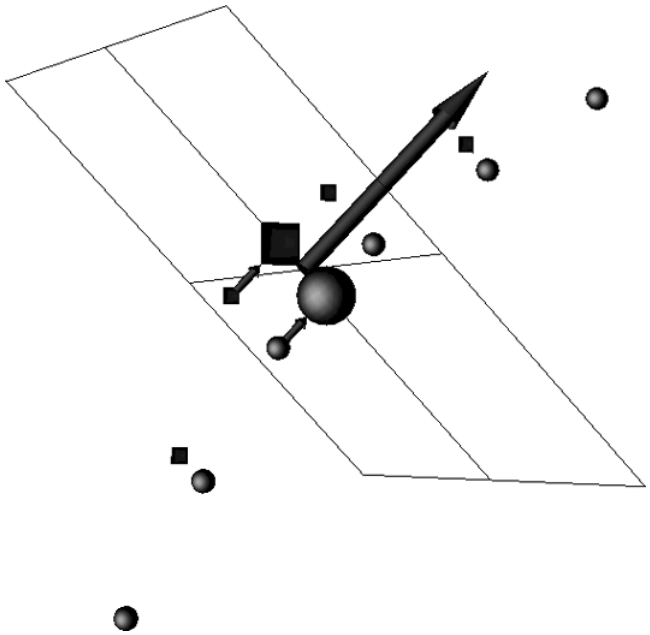

Figure 2. Cartoon of the construction of the mean line points and tangents. The base of the large rocket is placed at the mean of the resampled points, and the point of the large rocket illustrates the tangent. This becomes the normal to the plane, and the points on the unresampled line are relaxed onto the plane, illustrated by the small rockets.

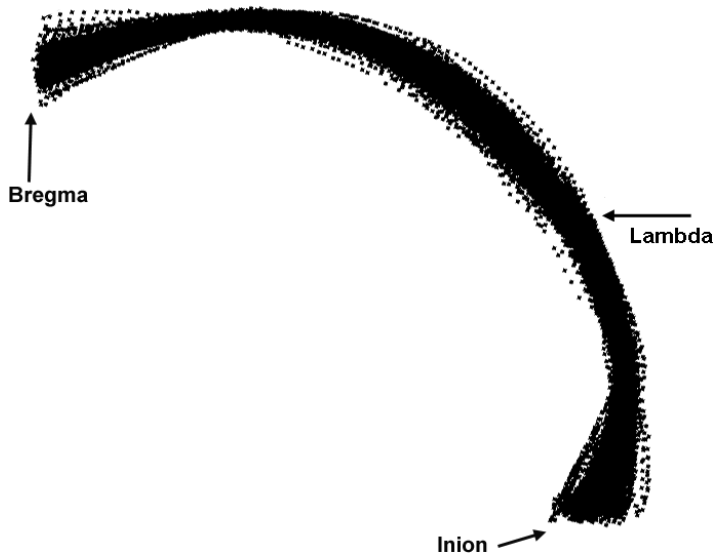

Figure 3. The unresampled points projected into the space of the resampled and Procrustes aligned points.

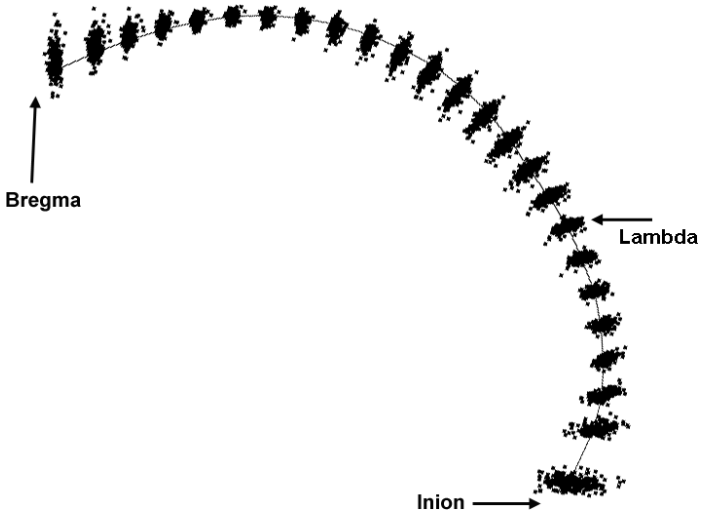

Figure 4. The resampled points and the mean line.

Next, the projection λ of each point in each of the unresampled curves on the perpendicular planes was calculated as

$$\lambda = n^{\mathrm{T}}(c - d)$$

where c is the pivot point of the plane, n is the normal, and d is successively each point in the curve. The point closest to the plane, namely the one having the minimum magnitude of λ, was then projected onto the plane, the projection z being

$$z = d_{\min} + \lambda_{\min} n$$

These steps applied to the actual data and the final result can be seen in Figures 3, 4, and 5.

It should be noted here that for curves whose trajectories are very convoluted, this definition of "closest" can fail, as the curves may cross the infinite perpendicular planes more than once, hence a more sophisticated test incorporating proximity would have to be devised. Also, we took the projection of the closest point onto the plane as an approximation of the intersection of the curve segment crossing each plane with the plane itself. In cases where the original, unresampled curves are perhaps less densely sampled than in the present study, this procedure could introduce errors, and it would then be advisable to correctly calculate the intersection, a more expensive calculation.

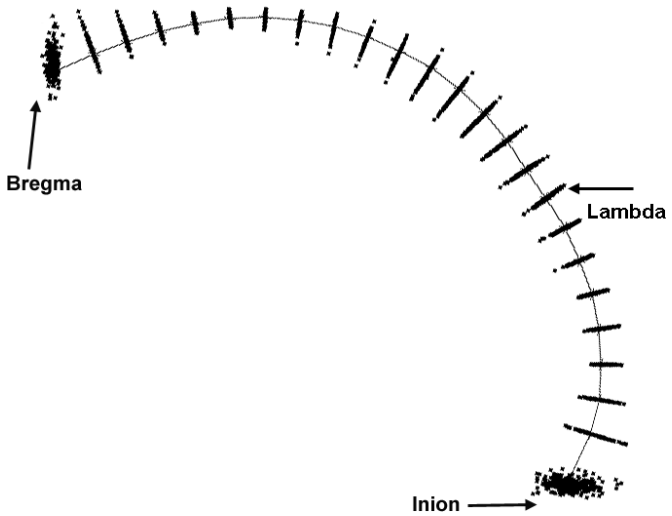

Figure 5. The nonuniform curve relaxation points and the mean line.

We here coin a term for this entire procedure, which we will call "nonuniform curve relaxation," to indicate that the relaxation in the bending energy (the reduction in extraneous variance) comes from choosing points at which the unresampled (nonuniformly sampled) curves intersect planes that are orthogonal to the tangent of the mean curve, rather than from sliding points along the tangents or splines of uniformly sampled curves.

In order to more directly compare results with our previous study of this material, which used two-dimensional curves limited to the mean sagittal plane, the three-dimensional curve segments were then reduced to two dimensions, using a singular value decomposition. The dimension with the lowest variance, the third or Z dimension in this case, was dropped, leaving only $X\Upsilon$ coordinates projected into the approximate mid-sagittal plane of each specimen.

RESULTS

A detailed presentation of the statistical analysis of the sliding data set, including discussion of each of the Neanderthal, pre-Neanderthal, and Late Paleolithic specimens appears elsewhere (Harvati and Reddy, in prep.) and should be consulted. The results presented here focus only on the salient differences between the two methods.

Principal Components Analysis

The two PCAs were similar in their results (Figures 6 and 7). In both analyses PC 1 (53.2% and 60.8% of total variance respectively for the *sliding* and *nonuniform curve relaxation data sets*) did not separate Neanderthals completely from modern humans. Along this component, Neanderthals were significantly different in their PC scores from all modern human populations except Late Paleolithic in the *sliding data set*; and from all modern humans except Late Paleolithic Europeans and Inugsuk Eskimos in the *nonuniform curve relaxation data set* (Bonferroni t-test). PC 2 (25.1% and 22.5% respectively) did separate Neanderthals from modern humans more completely in both analyses. Neanderthals were significantly different in their PC 2 scores from all modern human populations in both cases.

In both PCAs two of the Near Eastern Neanderthals fell well within the modern human range along PC 2: Shanidar 1 and Tabun C1. Furthermore,

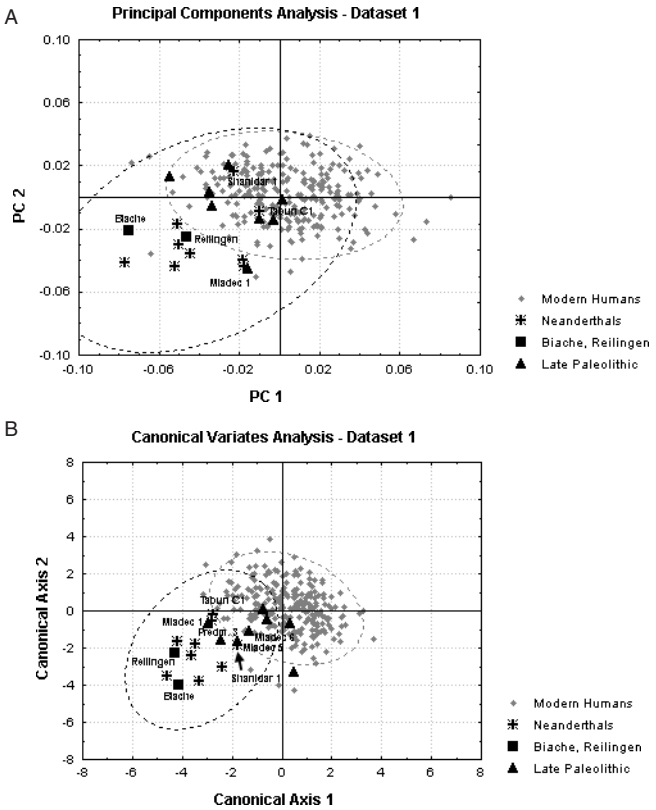

Figure 6. PCA and CVA for the sliding data set.

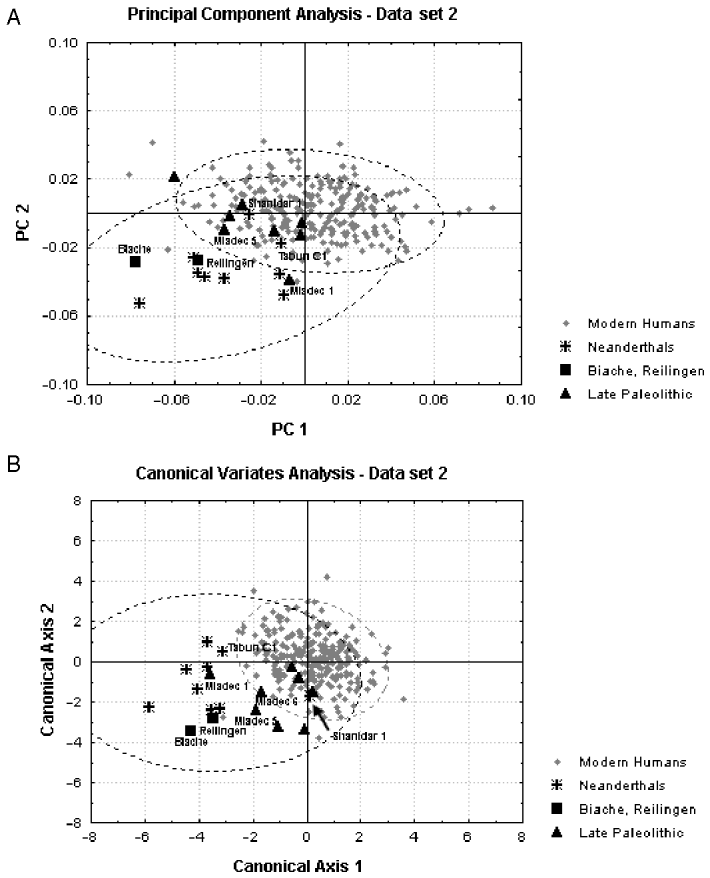

Figure 7. PCA and CVA for the nonuniform curve relaxation data set.

in both analyses one Upper Paleolithic specimen, Mladec 1, fell at the extreme of the modern human range and with Neanderthals on PC 2. Both pre-Neanderthal specimens fell with Neanderthals.

Canonical Variates Analysis

For both the sliding and the nonuniform curve relaxation data sets a CVA was performed on the first 15 principal components (99.5% and 99.3% of the total variance respectively, Figures 6 and 7), and using population rather than species as grouping variable. In both cases the first canonical axis (30.6% and 19.7% of the total variance respectively) separated Neanderthals from modern humans. Neanderthals were significantly different in their scores from all modern human populations along this axis.

The CVAs differ in that: in the *sliding CVA*, Shanidar 1 and Tabun C1 fell very close to each other at the end of the Neanderthal range and close to modern humans along Can 1 (Figure 6). Furthermore, in the sliding analysis, three Upper Paleolithic specimens fell in the area of overlap between Neanderthals and modern humans along Can 1 (Mladec 1 and 5 and Predmost 3). Mladec 6 was also close to the two Near Eastern Neanderthal specimens. The two pre-Neanderthal individuals fell with the Neanderthals. In the *nonuniform curve relaxation analysis*, Shanidar 1 fell well within the modern human range, whereas Tabun C1 did not. All the Late Paleolithic specimens fell in the area of overlap between Neanderthals and modern humans, due to the position of Shanidar 1. However, it has been suggested that this specimen may be artificially deformed (Trinkaus, 1982). Among the Late Paleolithics, the only specimen that fell within the rest of the Neanderthals along the first canonical axis 1 was Mladec 1.

AQ: Trinkaus, 1982 not listed in referneces

Mahalanobis Squared Distances

The Mahalanobis squared distances were calculated using a correction for unequal sample sizes (Marcus, 1993), and are presented in Tables 1 and 2. The two matrices are very similar. The general dichotomy between Neanderthals and modern humans was evident in both. In both analyses the pre-Neanderthal specimens were very close to each other, with Biache also being closest to Neanderthals while Reilingen was about equidistant from Neanderthals and the modern human populations. The *nonuniform curve relaxation data set* Mahalanobis squared distance matrix differed in that the distance between Neanderthals and the Late Paleolithic specimens was somewhat greater than that found when the sliding data set was used. This Neanderthal-to-Late Paleolithic distance was still the smallest distance between Neanderthals and modern humans, although it was now almost equal to the Neanderthal–Khoisan distance.

Discriminant Analysis

When treated as unknown specimens to be classified by posterior probability in a discriminant analysis, in the *sliding data set*: Mladec 1 was the only Late Paleolithic specimen classified as Neanderthal when asked to classify to population. In this analysis, Shanidar 1 was classified as modern human (Inugsuk Eskimo).

Table 1. Bias-corrected Mahalanobis squared distances matrix for the sliding data set

	Nea	And	Aus	Brg	Dgn	Epi	Esk	Eur	LP	San	Tol	Bch	Reil
Nea	0.00												
And	20.95	0.00											
Aus	18.43	4.63	0.00										
Brg	21.32	4.04	6.83	0.00									
Dgn	16.90	4.38	5.66	10.35	0.00								
Epi	20.93	1.33	3.32	3.70	6.74	0.00							
Esk	13.62	4.25	4.90	3.18	7.20	4.70	0.00						
Eur	18.42	2.29	6.84	NS0.39	7.86	3.10	2.77	0.00					
LP	10.06	8.64	4.87	7.24	9.81	8.63	7.73	6.97	0.00				
San	12.97	2.53	4.39	5.84	2.33	4.23	4.28	4.70	7.17	0.00			
Tol	20.72	2.79	5.71	3.43	6.31	4.43	2.97	2.99	10.04	4.89	0.00		
Bch	NS2.57	38.58	32.13	34.68	33.03	34.91	24.43	32.35	19.20	31.30	34.41	0.00	
Reil	37.65	57.98	44.58	54.17	48.32	49.8	52.26	55.30	37.65	52.33	60.17	NS11.17	0.00

Note: Nea: Neanderthal; And: Andaman Islanders; Aus: Australian; Brg: Austrian Berg; Dgn: W. African Dogon; Epi: Afalou/Taforalt; Esk: Inugsuk Eskimo; Eur: W. Eurasian; LP: Late Paleolithic; San: Khoisan; Tol: Melanesian Tolai; Bch: Biache; Reil: Reilingen.

Table 2. Bias-corrected Mahalanobis squared distances matrix for the nonuniform curve relaxation data set (group labels as in Table 1)

	Nea	And	Aus	Brg	Dgn	Epi	Esk	Eur	LP	San	Tol	Bch	Reil
Nea	0.00												
And	19.51	0.00											
Aus	14.15	2.99	0.00										
Brg	18.53	3.84	3.07	0.00									
Dgn	14.45	3.45	5.08	7.49	0.00								
Epi	20.31	3.02	2.39	1.75	6.11	0.00							
Esk	15.06	4.27	3.34	1.94	5.59	5.09	0.00						
Eur	17.67	3.10	3.65	NS0.57	5.57	3.06	2.62	0.00					
LP	11.03	10.48	4.60	6.63	11.10	8.40	7.21	4.94	0.00				
San	11.63	4.55	3.05	5.72	1.72	4.52	4.08	4.61	7.56	0.00			
Tol	18.34	2.00	3.60	2.29	5.05	4.27	1.76	2.81	11.37	5.25	0.00		
Bch	NS9.67	40.44	37.57	34.79	37.67	41.55	32.29	35.17	23.89	35.69	38.02	0.00	
Reil	46.58	58.28	56.12	53.59	57.01	58.59	61.19	59.43	45.98	58.07	62.04	NS19.33	0.00

When asked to classify to species, Mladec 1, 5, and 6, as well as Predmost 3, were classified as Neanderthals; whereas Shanidar 1 was classified as Neanderthal. Both pre-Neanderthals were classified as Neanderthal in both instances. A cross-validation classification performed on the entire data set succeeded in classifying eight out of the nine (88.9%) Neanderthal specimens and 249 of the 255 (97.6%) modern human specimens to species correctly.

With the *nonuniform curve relaxation data set*, when asked to classify to population, Mladec 1 was classified as Neanderthal and Shanidar 1 was classified as modern human (Austrian Berg). When asked to classify to species, Mladec 1 and 6, but not 5, were also classified as Neanderthals. Unlike with the sliding data set, Shanidar 1 was now classified incorrectly as modern human when asked to classify to species. In both discriminant analyses the pre-Neanderthal specimens were classified as Neanderthal. The cross-validation classification succeeded in classifying seven out of the nine (77.8%) Neanderthal specimens and 253 of the 255 (99.2%) modern human specimens to species correctly.

CONCLUSIONS

Sub-sampling curves to achieve uniform sampling is inherently a low pass filtering operation, reducing the local, high-frequency information inherent in the original, nonuniformly sampled curve data. Nonuniform curve relaxation, by taking this local, high-frequency information into consideration when constructing relaxed, uniformly sampled curves, can help to preserve subtle features of the curves through resampling. It avoids the degradation of signal quality that occurs when sub-sampling is performed first and the curves are subsequently relaxed based on their reduced information content. The true strength of the technique lies in combining the uniform resampling and the relaxation, or sliding, process into one optimized algorithm and in treating the set of curves as a whole. In contrast, standard techniques apply sub-sampling to the individual curves, reducing their information content, and then apply relaxation as a statistical correction.

Nonuniform curve relaxation may be an attractive alternative to sliding for better preserving subtle shape information, which may in turn reduce misclassification of individual specimens. Although in this case the results of the two analyses did not differ dramatically, we feel that the increased accuracy of the data does result in fewer inconsistencies in the analysis of the occipital bun shape. The nonuniform curve relaxation analysis did result in somewhat

greater discrimination between modern humans with posterior cranial profile shapes similar to, yet subtly different from, Neanderthals and the true Neanderthal specimens. On the other hand, some of the Late Paleolithic specimens were consistent in showing similarities to the Neanderthal sample. Finally, the Near Eastern Neanderthal Shanidar 1 was consistently found in the nonuniform curve relaxation analysis to fall with modern humans in all statistical analyses, underscoring the problematic nature of the posterior cranial profile of this individual. These results and their implications for the relationship between Neanderthals and early modern humans are explored further in Harvati and Reddy (in prep.).

REFERENCES

Bookstein, F. L., 1989, Principal warps: Thin-plate splines and the decomposition of deformations. *IEEE Trans. Patt. Anal. Mach. Intell.* 11:567–585.

Bookstein, F. L., *Morphometric Tools for Landmark Data*. Cambridge Press, Cambridge, 435 pp.

Bookstein, F. L., 1997, Landmark methods for forms without landmarks: Localizing group differences in outline shape, *Med. Image. Anal.* 1:225–243.

Bookstein, F. L., Schaefer, K., Prossinger, H., Seidler, H., Fieder, M., Stringer, M., Weber, G. et al., 1999, Comparing frontal cranial profiles in archaic and modern Homo by morphometric analysis, *Anat. Rec.* (*New Anat.*) 257:217–224.

Dean, D., 1993, The middle Pleistocene *Homo erectus/Homo sapiens* transition: New evidence from space curve statistics, Ph.D. dissertation, City University of New York, New York.

AQ: Dean, 1993 not cited in text

Dean, D., Hublin, J. J., Holloway, R., and Ziegler, R., 1998, On the phylogenetic position of the pre-Neanderthal specimen from Reilingen, Germany, *J. Hum. Evol.* 34:485–508.

Ducros, A., 1967, Le chignon occipital, mesure sur le squelette, *L'Anthropologie* 71:75–96.

Harvati, K., 2001, The Neanderthal problem: 3-D geometric morphometric models of cranial shape variation within and among species, Ph.D. dissertation, City University of New York, New York.

Harvati, K., Reddy, D. P., and Marcus L. F., 2002, Analysis of the posterior cranial profile morphology in Neanderthals and modern humans using geometric morphometrics, *Am. J. Phys. Anthropol.* S34:83.

Harvati, K. and Reddy, D. P., in prep., Quantitative assessment of the Neanderthal occipital "bun" using geometric morphometric ridge-curve analysis.

Marcus, L. F., 1993, Some aspects of multivariate statistics for morphometrics, in: L. Marcus, F. Bello, and A. García-Valdecasas, eds., Contributions to Morphometrics, Madrid: Monografias Museo Nacional de Ciencias Naturales, pp. 99–130.

Marcus, L. F., Frost, S. R., Bookstein, F. L., Reddy, D. P., and Delson, E., 2000, *Comparison of Landmarks among Living and Fossil Papio and Theropithecus skulls, with Extension of Procrustes Methods to Ridge Curves*, completed manuscript, http://research.amnh.org/nycep/aapa99/aapa6.html, 2000.

Strang G., 1976, *Linear Algebra and its Applications*, Academic Press, New York, pp. 106–107.